

A Chelating N-Heterocyclic Carbene Ligand in Organochromium Chemistry

Kevin A. Kreisel, Glenn P. A. Yap, and Klaus H. Theopold*

Department of Chemistry and Biochemistry, Center for Catalytic Science and Technology,
University of Delaware, Newark, Delaware 19716

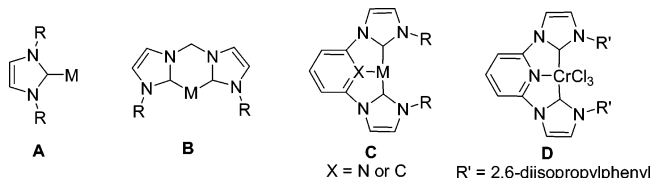
Received June 9, 2006

Several chromium complexes supported by a chelating N-heterocyclic carbene ligand have been prepared in an attempt to study their ability to catalyze the polymerization of ethylene. $\text{LCrCl}_3(\text{THF})$ (**3**) ($\text{L} = 1,1'$ -methylene-3,3'-di-2,6-diisopropylphenylimidazole-2,2'-diylidene (**2**)) was found to polymerize ethylene when activated by either excess methylaluminumoxane (MAO) or excess Et_2AlCl . Chloride abstraction from **3** with Na^+BARF^- ($\text{BARF}^- = \text{tetrakis}(3,5\text{-di-trifluoromethylphenyl})\text{borate}$) yielded a dinuclear, chloride-bridged product, $[(\text{LCrCl})_2(\mu\text{-Cl})_3]^+\text{BARF}^-$ (**4**). In a similar fashion, reaction of **3** with 3.0 equiv of AlMe_3 gave the dinuclear, chloride-bridged alkyl cation $[(\text{LCrMe})_2(\mu\text{-Cl})_3]^+\text{AlX}_4^-$ ($\text{X} = \text{Me}, \text{Cl}$) (**5**), which is isostructural to **4**. A triaryl complex was also prepared by reaction of **2** with $\text{CrPh}_3(\text{THF})_3$, giving LCrPh_3 (**6**) in good yield. Similarly, a series of alkyl and aryl chloride complexes of the form $\text{LCrCl}_2(\text{THF})$ ($\text{R} = \text{Me}$ (**7a**), Ph (**7b**), tolyl (**7c**)) have also been made from the appropriate $\text{CrRCl}_2(\text{THF})_3$ starting material. Further treatment of **7a** with Na^+BARF^- resulted in the formation of the BARF^- salt of complex **5**. Complexes **3–6** and **7a–c** catalyze the polymerization of ethylene when activated by MAO. Preliminary studies with Cr(II) have shown that $\text{LCrX}_2(\text{THF})$ ($\text{X} = \text{Cl}$ (**8a**), Br (**8b**)) does not polymerize ethylene upon activation by either MAO or alkylaluminum reagents. Complexes **3–6**, **7c**, and **8b** have been structurally characterized by X-ray diffraction methods.

Introduction

N-Heterocyclic carbene (NHC) ligands have recently become popular alternatives to phosphines due to their strong σ -donating and poor π -accepting character, ease of changing steric bulk, and lower toxicity.¹ This combination of properties has prompted their use as ligands for numerous transition metals, and their metal complexes have proven successful in a variety of catalytic reactions.² Complexes **A–C** in Scheme 1 show a generic set of reported NHC complexes. A large number of reported examples contain one or more monodentate NHC ligands (**A**); only a small fraction contain bidentate NHCs (**B**).³ Recently the interest in the chemistry of CXC pincer ligands (**C**) has increased ($\text{X} = \text{C}$ or N), yet few have been shown to be active for catalytic transformations.⁴ However, Gibson et al. have

Scheme 1



shown that a chelating NHC pincer complex of chromium(III) (**D**) is very active as an ethylene oligomerization catalyst in the presence of excess methylaluminumoxane (MAO).⁵

We have been interested in the polymerization of ethylene using homogeneous chromium catalysts supported by a variety of ancillary ligands, e.g., cyclopentadienyl (Cp) and its derivatives⁶ and β -diketiminates (nacnac).⁷ We hoped to expand our investigation to chelating NHC ligands and their potential as ancillary ligands for chromium-mediated ethylene polymeriza-

* To whom correspondence should be addressed. E-mail: theopold@udel.edu.

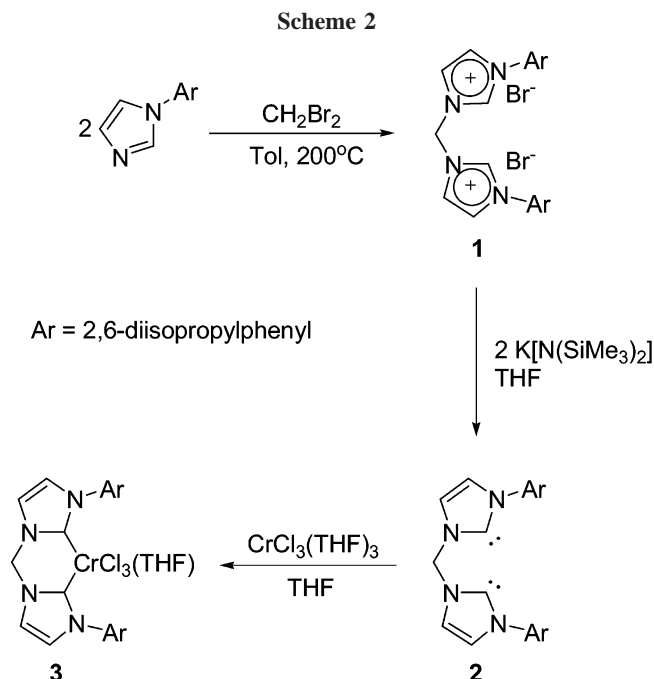
(1) (a) Waltman, A. W.; Grubbs, R. H. *Organometallics* **2004**, *23*, 3105. (b) Dharmasena, U. L.; Foucault, H. M.; dos Santos, E. N.; Fogg, D. E.; Nolan, S. P. *Organometallics* **2005**, *24*, 1056. (c) Hu, X.; Castro-Rodriguez, I.; Olsen, K.; Meyer, K. *Organometallics* **2004**, *23*, 755. (d) Dorta, R.; Stevens, E. D.; Hoff, C. D.; Nolan, S. P. *J. Am. Chem. Soc.* **2003**, *125*, 10490. (e) Nakai, H.; Hu, X.; Zakharov, L. N.; Rheingold, A. L.; Meyer, K. *Inorg. Chem.* **2004**, *43*, 855. (f) Castarlenas, R.; Esteruelas, M. A.; Onate, E. *Organometallics* **2005**, *24*, 4343. (g) Buchgraber, P.; Toupet, L.; Guerschais, V. *Organometallics* **2003**, *22*, 5144. (h) Caddick, S.; Cloke, F. G. N.; Hitchcock, P. B.; Lewis, A. K. D. *Angew. Chem., Int. Ed.* **2004**, *43*, 5824. (i) Danopoulos, A. A.; Hankin, D. M.; Wilkinson, G.; Cafferkey, S. M.; Sweet, T. K. N.; Hursthouse, M. B. *Polyhedron* **1997**, *16*, 3879. (j) Voges, M. H.; Rømming, C.; Tilset, M. *Organometallics* **1999**, *18*, 529.

(2) (a) Herrmann, W. A. *Angew. Chem., Int. Ed.* **2002**, *41*, 1291, and references therein. (b) Bielański, C. W.; Grubbs, R. H. *Angew. Chem., Int. Ed.* **2000**, *39*, 2903. (c) Frenzel, U.; Weskamp, T.; Kohl, F. J.; Schattenmann, O. N.; Herrmann, W. A. *J. Organomet. Chem.* **1999**, *586*, 263. (d) Döhning, A.; Göhre, J.; Jolly, P. W.; Kryger, B.; Rust, J.; Verhovnik, G. P. *J. Organometallics* **2000**, *19*, 388. (e) Frey, G. D.; Schutz, J.; Herdtweck, E.; Herrmann, W. A. *Organometallics* **2005**, *24*, 4416. (f) Gstottmayr, C. W. K.; Bohm, V. P. W.; Herdtweck, E.; Gosche, M.; Herrmann, W. A. *Angew. Chem., Int. Ed.* **2002**, *41*, 1363.

(3) (a) Clyne, D. S.; Jin, J.; Genest, E.; Gallucci, J. C.; RajanBabu, T. V. *Org. Lett.* **2000**, *2*, 1125. (b) Douthwaite, R. E.; Green, M. L. H.; Silcock, P. J.; Gomes, P. T. *Organometallics* **2001**, *20*, 2611. (c) Vogt, M.; Pons, V.; Heinekey, D. M. *Organometallics* **2005**, *24*, 1832. (d) Herrmann, W. A.; Schwarz, J.; Gardiner, M. G. *Organometallics* **1999**, *18*, 4082. (e) Quezada, C. A.; Garrison, J. C.; Tessier, C. A.; Youngs, W. J. *J. Organomet. Chem.* **2003**, *671*, 183. (f) Herrmann, W. A.; Schwarz, J.; Gardiner, M. G.; Spiegler, M. *J. Organomet. Chem.* **1999**, *575*, 80.

(4) (a) Danopoulos, A. A.; Tsoureas, N.; Wright, J. A.; Light, M. E. *Organometallics* **2004**, *23*, 166. (b) Simons, R. S.; Custer, P.; Tessier, C. A.; Youngs, W. J. *Organometallics* **2003**, *22*, 1979. (c) Grundemann, S.; Albrecht, M.; Loch, J. A.; Faller, J. W.; Crabtree, R. H. *Organometallics* **2001**, *20*, 5485. (d) Poyatos, M.; Mata, J. A.; Falomir, E.; Crabtree, R. H.; Peris, E. *Organometallics* **2003**, *22*, 1110. (e) Loch, J. A.; Albrecht, M.; Peris, E.; Mata, J.; Faller, J. W.; Crabtree, R. H. *Organometallics* **2002**, *21*, 700. (f) Mas-Marzá, E.; Saná, M.; Peris, E. *J. Organomet. Chem.* **2005**, *690*, 5576.

(5) (a) McGuinness, D. S.; Gibson, V. C.; Wass, D. F.; Steed, J. W. *J. Am. Chem. Soc.* **2003**, *125*, 12716. (b) McGuinness, D. S.; Gibson, V. C.; Steed, J. W. *Organometallics* **2004**, *23*, 6288.



tion. Unlike Gibson's η^3 NHC pincer complexes mentioned above, we have used a bidentate bis(NHC), which binds solely through two carbene carbons (**B** in Scheme 1). Previous work with this ligand and chromium featured chromium(0), but the scope of the investigation was not extensive.⁸ Herein we report our work on the organometallic chemistry of chromium(III and II) using the NHC ligand 1,1'-methylene-3,3'-di-2,6-diisopropylphenylimidazole-2,2'-diylidene.

Results and Discussion

Our foray into the chromium chemistry of the bidentate NHC ligand began with the preparation of the imidazolium salt by an adaption of previously reported procedures:⁹ heating 2 equiv of 2,6-diisopropylphenylimidazole with 1 equiv of CH_2Br_2 to 200°C in a closed ampule for 3 days (Scheme 2). The ^1H NMR spectrum of the resulting bis-imidazolium dibromide salt ($[\text{LH}_2]\text{Br}_2$, **1**) in $\text{DMSO}-d_6$ showed a characteristic singlet at 10.57 ppm, which was assigned to the protons at the 2-positions of the imidazolium rings. The ^{13}C NMR spectrum showed a characteristic peak at 58.69 ppm, which was attributed to the bridging methylene carbon. The solid-state structure of **1** has been determined by X-ray diffraction and is depicted in Figure 1; selected interatomic distances and angles can be found in Table 1. **1** crystallizes in the orthorhombic space group $Pbcn$

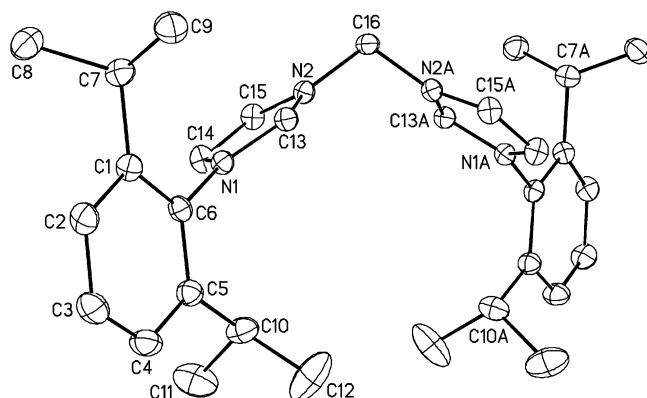


Figure 1. ORTEP plot of the bis(imidazolium) dibromide salt (**1**) at the 30% probability level. The bromide counterions and hydrogen atoms have been omitted for clarity.

Table 1. Selected Interatomic Distances (Å) and Angles (deg) for the Bis(imidazolium) Dibromide Salt (**1**)

N(1)–C(13)	1.328(5)	N(2)–C(15)	1.381(5)
N(1)–C(14)	1.387(5)	C(14)–C(15)	1.349(5)
N(2)–C(13)	1.336(4)	N(2)–C(16)–N(2A)	110.0(4)

and features a C_2 axis at the bridging methylene carbon. Retention of the tetrahedral geometry of the bridging methylene in **1** is evident in the $\text{N}(2)\text{--C}(16)\text{--N}(2\text{A})$ bond angle of $110.0(4)^\circ$, despite the bulky aryl groups at the 3-position of the imidazolium rings. The effect of delocalization of the π -electrons in the imidazolium ring can be detected in the C--N bond distances of 1.328(5)–1.387(5) Å as compared to the single-bond distance of the methylene carbon to the imidazolium nitrogen (1.462(4) Å).

Deprotonation of **1** with 2 equiv of $\text{K}[\text{N}(\text{SiMe}_3)_2]$ in THF according to Scheme 2 resulted in an initial color change to blue, followed by a gradual color change to brown. After workup, 1,1'-methylene-3,3'-di-2,6-diisopropylphenylimidazole-2,2'-diylidene (**2**) could be obtained in good yield (~70%) as a white to light yellow powder. The ^1H NMR spectrum of **2** in CD_2Cl_2 lacks the singlet at 10.57 ppm (proton at the 2-position of the imidazole ring) observed in the ^1H NMR of **1**. The ^{13}C NMR spectrum of **2** also shows a shift of the bridging methylene carbon in **1** to 65.72 ppm and the appearance of a peak at 219.01 ppm, indicative of the carbene carbon in the 2-position of the imidazole ring. **2** is air- and moisture-sensitive and can be easily converted back to the imidazolium salt by reaction with 2 equiv of HCl under anhydrous conditions.

Coordination of the free bis-carbene to $\text{Cr}(\text{III})$ was accomplished by the addition of **2** to a slurry of $\text{CrCl}_3(\text{THF})_3$ in THF at room temperature (Scheme 2). The resulting pale blue precipitate was surprisingly insoluble, necessitating recrystallization from hot THF. The solid-state structure of the product, $\text{LCrCl}_3(\text{THF})$ (**3**) ($\text{L} = \text{2}$), is shown in Figure 2. Selected interatomic distances and angles are listed in Table 2. Complex **3** crystallizes in the triclinic space group $P\bar{1}$, and the asymmetric unit contains two crystallographically distinct, but chemically equivalent molecules. The geometry around the Cr is almost perfectly octahedral, with the ligands *cis* to one another having bond angles ranging from $84.35(10)^\circ$ to $94.56(17)^\circ$ with an average angle of 90.01° . The bridging methylene carbon remains nearly tetrahedral and establishes a bond angle of $110.6(4)^\circ$ with respect to $\text{N}(2)$ and $\text{N}(3)$. The Cr--C bond length of 2.109(5) Å for $\text{Cr}(1)\text{--C}(17)$ is in the range of other reported Cr--NHC

(6) (a) Richeson, D. S.; Hsu, S. W.; Fredd, N. H.; Van Duyne, G.; Theopold, K. H. *J. Am. Chem. Soc.* **1986**, *108*, 1491. (b) Thomas, B. J.; Noh, S. K.; Schulte, G. K.; Sendlinger, S. C.; Theopold, K. H. *J. Am. Chem. Soc.* **1991**, *113*, 893. (c) Thomas, B. J.; Theopold, K. H. *J. Am. Chem. Soc.* **1988**, *110*, 5902. (d) Thomas, B. J.; Mitchell, J. F.; Leary, J. A.; Theopold, K. H. *J. Organomet. Chem.* **1988**, *348*, 333. (e) White, P. A.; Calabrese, J.; Theopold, K. H. *Organometallics* **1996**, *15*, 5473. (f) Liang, Y.; Yap, G. P. A.; Rheingold, A. L.; Theopold, K. H. *Organometallics* **1996**, *15*, 5284.

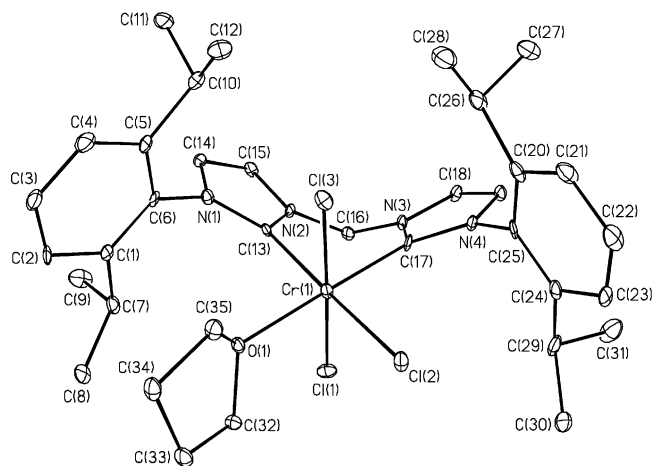
(7) (a) Kim, W.; Fevola, M. J.; Liable-Sands, L. M.; Rheingold, A. L.; Theopold, K. H. *Organometallics* **1998**, *17*, 4541. (b) MacAdams, L. A.; Kim, W.; Liable-Sands, L. M.; Guzei, I. A.; Rheingold, A. L.; Theopold, K. H. *Organometallics* **2002**, *21*, 952. (c) MacAdams, L. A.; Buffone, G. P.; Incarvito, C. D.; Rheingold, A. L.; Theopold, K. H. *J. Am. Chem. Soc.* **2005**, *127*, 1082.

(8) Oefele, K.; Herrmann, W. A.; Mihalios, D.; Elison, M.; Herdtweck, E.; Priemeier, T.; Kiprof, P. *J. Organomet. Chem.* **1995**, *498*, 1.

(9) Douthwaite, R. E.; Haüssinger, D.; Green, M. L. H.; Silcock, P. J.; Gomes, P. T.; Martins, A. M.; Danopoulos, A. A. *Organometallics* **1999**, *18*, 4584.

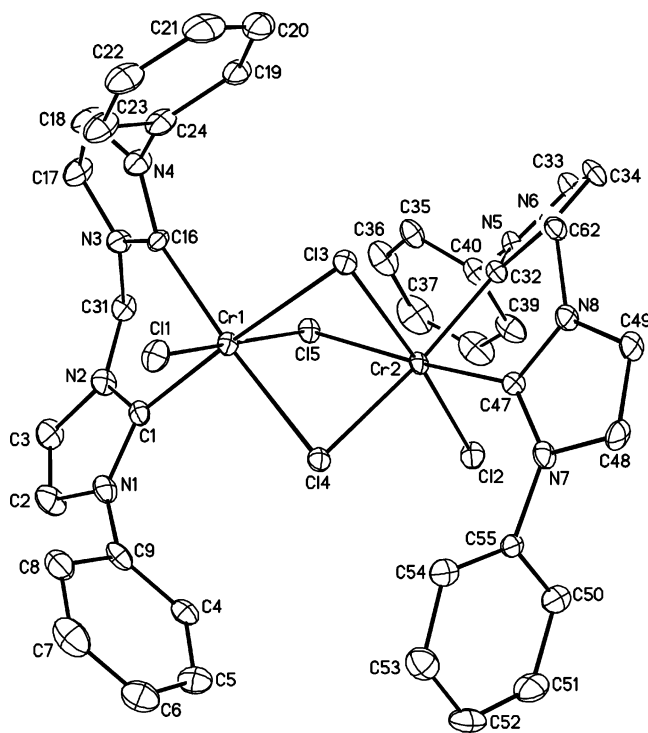
Table 2. Selected Interatomic Distances (Å) and Angles (deg) for One of the Two Independent Molecules of $\text{LCrCl}_3(\text{THF})$ (**3**)

N(1)–C(13)	1.367(6)	Cr(1)–C(17)	2.109(5)	C(13)–Cr(1)–Cl(2)	178.50(15)
N(1)–C(14)	1.390(6)	Cr(1)–Cl(1)	2.3444(17)	C(13)–Cr(1)–O(1)	94.56(17)
N(2)–C(13)	1.353(6)	Cr(1)–Cl(2)	2.3241(17)	C(17)–Cr(1)–O(1)	179.30(19)
N(2)–C(15)	1.387(6)	Cr(1)–Cl(3)	2.2803(17)	Cl(1)–Cr(1)–Cl(3)	176.90(7)
C(14)–C(15)	1.342(7)	Cr(1)–O(1)	2.163(3)	Cl(1)–Cr(1)–Cl(2)	91.45(6)
Cr(1)–C(13)	2.134(5)	C(13)–Cr(1)–C(17)	85.9(2)	Cl(2)–Cr(1)–O(1)	86.70(10)

**Figure 2.** ORTEP plot of $\text{LCrCl}_3(\text{THF})$ (**3**) at the 30% probability level. Hydrogen atoms have been omitted for clarity.

complexes,^{1j,5a,10} but the carbene *trans* to Cl(2) is considerably longer at 2.134(5) Å and is on the longer end of all reported metal–NHC complexes (av = 2.073 Å).¹¹ The Cr–Cl distances are in the range of other reported Cr(III)–Cl distances,¹² which range from 2.280(2) to 2.344(2) Å in **3**. Comparison of the bond distances in the imidazole rings between **1** and **3** shows an increase in the bond length of N(1)–C(13) and N(2)–C(13) to 1.367(6) and 1.353(6) Å, respectively, and relatively little change in the distance for C(14)–C(15) (1.342(7) Å), thus showing the loss of the delocalization of the π -electrons in the imidazole rings. Interestingly, the chloride ligand *trans* to the NHC ligand, Cl(2), shows no sign of a significant *trans* influence exerted by the strongly σ -donating NHC ligand with the Cr(1)–Cl(2) bond length being intermediate in length of the three metal–chloride bonds. The THF ligand coordinated to the Cr in **3** has a bond length of 2.163(3) Å, which is in the range of other THF-coordinated complexes of Cr(III).¹³ Complex **3** exhibits a room-temperature effective magnetic moment of 4.0(1) μ_B , consistent with a d^3 ion having three unpaired electrons ($S = 3/2$).

The coordinated THF in **3** is apparently quite labile, which could be attributed to a *trans* influence by the NHC ligand, and simply exposing the complex to vacuum or suspending it in a solvent other than THF (i.e., Et_2O , CH_2Cl_2 , toluene, pentane) resulted in an immediate color change to green. Upon placing the green complex back in THF, the complex immediately reverted back to the blue, THF-coordinated, **3**. Because of the ease of removal of the coordinated solvent, it was difficult to

**Figure 3.** ORTEP plot of $(\text{LCrCl})_2(\mu\text{-Cl})_3^+\text{BARF}^-$ (**4**) at the 30% probability level. The BARF counterion, hydrogen atoms, and the 2,6-diisopropyl groups of the phenyl rings have been omitted for clarity.

quantify the amount of THF that was released. Accordingly, the elemental analysis of **3** is slightly low for the content of carbon (see Experimental Section). The reactivity of **3**, in some sense, is influenced by the apparent lability of the coordinated THF.

In an attempt to determine if chloride abstraction from **3** is plausible, Na^+BARF^- (BARF = tetrakis(3,5-di-trifluoromethylphenyl)borate) was added to a THF solution of **3**, giving the green binuclear complex $[(\text{LCrCl})_2(\mu\text{-Cl})_3]\text{BARF}$ (**4**) after 6 h at room temperature (Scheme 3). When the same reaction was run in Et_2O , the conversion from **3** to **4** was instant. The difference in the apparent rates may be attributed to inhibition of ligand dissociation by the THF solvent. Crystals of **4** were grown from Et_2O at -30°C , and the result of the X-ray structure determination is shown in Figure 3, with interatomic distances and angles listed in Table 3.

Complex **4** also crystallizes in the triclinic space group $P\bar{1}$. It consists of two Cr atoms, coordinated by one terminal chloride each and bridged by three chlorides, one of which, Cl(4), lies on a noncrystallographically imposed, pseudo- C_2 axis. The complex is cationic and comes with a noninteracting BARF^- counterion. The coordination geometry around each Cr in **4** is distorted octahedral, with the N atoms of the chelating NHC ligand on Cr(1) coplanar with Cl(3) and Cl(4) and the NHC of Cr(2) coplanar with Cl(4) and Cl(5). Carbene carbons C(16) and C(32) are nearly eclipsed, with a torsion angle of only 8.3-(2)°, whereas the other two carbenes have a dihedral angle of

(10) Abernethy, C. D.; Clyburne, J. A. C.; Cowley, A. H.; Jones, R. A. *J. Am. Chem. Soc.* **1999**, *121*, 2329.

(11) Allen, F. H. *Acta Crystallogr.* **2002**, *B58*, 380.

(12) (a) Carney, M. J.; Robertson, N. J.; Halfen, J. A.; Zakharov, L. N.; Rheingold, A. L. *Organometallics* **2004**, *23*, 6184. (b) Baker, R. J.; Davies, P. C.; Edwards, P. G.; Farley, R. D.; Liyanage, S. S.; Murphy, D. M.; Yong, B. *Eur. J. Inorg. Chem.* **2002**, 1975. (c) Kohn, R. D.; Haufe, M.; Kociok-Kohn, G.; Grimm, S.; Wasserscheid, P.; Keim, W. *Angew. Chem., Int. Ed.* **2000**, *39*, 4337.

(13) (a) Bazan, G. C.; Rogers, J. S.; Fang, C. C. *Organometallics* **2001**, *20*, 2059. (b) Bhandari, G.; Kim, Y.; McFarland, J. M.; Rheingold, A. L.; Theopold, K. H. *Organometallics* **1995**, *14*, 738. (c) Dionne, M.; Jubb, J.; Jenkins, H.; Wong, S.; Gambarotta, S. *Inorg. Chem.* **1996**, *35*, 1874.

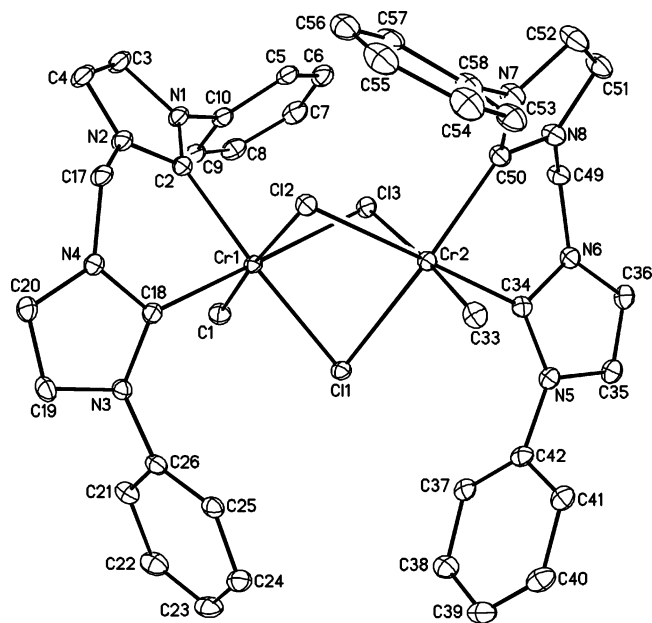


Figure 4. ORTEP plot of $(\text{LCrMe})_2(\mu\text{-Cl})_3^+\text{BARF}^-$ (**5**) at the 30% probability level. The BARF counterion, hydrogen, and the 2,6-diisopropyl groups of the phenyl rings atoms have been omitted for clarity.

about 120° . The Cr–carbene distances are similar to those in **3**, the terminal Cr–Cl distances are normal, and, as expected, the bridging chlorides (2.3702(15) to 2.4101(15) Å) have longer Cr–Cl distances than the terminal chlorides (2.2433 and 2.2419 Å).¹⁴ Similarly to **3**, complex **4** does not show any sign of a *trans* influence on the chloride ligands; the chloride that lies on the C_2 axis, Cl(4), which is the only chloride *trans* to two carbenes, has the shortest Cr–Cl distances of the bridging chlorides.

This $(\text{CrCl})_2(\mu\text{-Cl})_3$ core is not a familiar structural motif for Cr(III), and a search of the Cambridge Structural Database returned only one hit for Cr in this structural setting.¹⁵ Since Cr(III) is not known for its propensity to form metal–metal bonds (the Cr–Cr distance in **4** is 3.1116(12) Å), it must be the desire for Cr(III) to be octahedral that is the thermodynamic driving force to give **4**.¹⁶ Further evidence for the +3 oxidation state of Cr and the absence of a Cr–Cr interaction is given by the room-temperature effective magnetic moment of 3.6(1) μ_B per Cr, which is consistent with the three unpaired electrons of octahedral Cr(III).

Treatment of **3** with AlMe_3 as an alkylating agent in THF resulted in a color change to red over the course of an hour (Scheme 3). Workup and recrystallization gave a bright red material, which we tentatively assign as $[(\text{LCrMe})_2(\mu\text{-Cl})_3]^+\text{AlX}_4^-$ ($X = \text{Me}, \text{Cl}$) because of the similarities in the ^1H NMR spectra of this complex and that of the BARF[−] salt (**5**), synthesized by a different route (vide infra). The formation of **4** and **5** via this chloride abstraction route suggests that halide abstraction from the chromium center leads to immediate dimerization, which seems to be a common occurrence in the chemistry of this system. Figure 4 shows the solid-state structure of **5**, and

Scheme 3

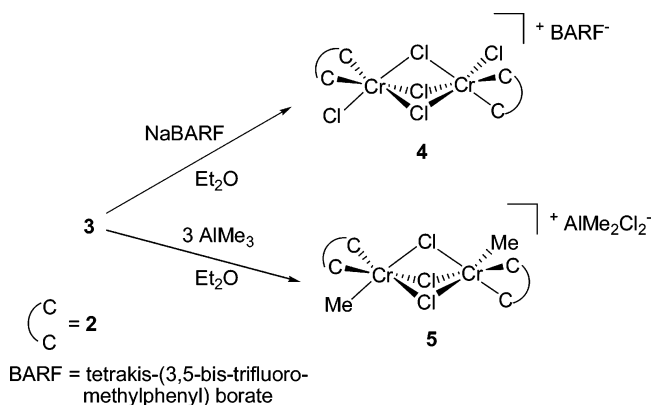


Table 4 provides selected bond lengths and angles. Complex **5** crystallizes in the triclinic space group $P\bar{1}$ with a C_2 axis on Cl(1). **4** and **5** are isostructural with the same $(\text{CrX})_2(\mu\text{-Cl})_3$ core ($X = \text{Cl}, \text{Me}$). Similar to **4**, complex **5** exhibits a distorted octahedral geometry, with the NHC ligand bound to Cr(1) being coplanar with Cl(1) and Cl(3) while the NHC ligand on Cr(2) is coplanar with Cl(1) and Cl(2). Like **4**, complex **5** has two carbene carbons that are eclipsed, with a C(2)–Cr(1)–Cr(2)–C(50) torsion angle of $5.9(6)^\circ$, while the other carbene torsion angle is close to 120° . The Cr–carbene distances are like those in **3** and **4**, and the distances from Cr to the bridging chlorides are all on par with **4**, although Cl(1), *trans* to two carbenes, has an increased Cr–Cl bond length of 2.3901(6) and 2.3917(6) Å compared to **4**. Cl(2) and Cl(3) do show signs of a *trans* influence from the terminal methyls C(1) and C(33), their bond lengths to Cr increasing to nearly 2.50 Å. The Cr–Me bond lengths of **5** (C(1) and C(33)) are 2.058(2) Å and are in the range of other Cr complexes with metal alkyl complexes (2.032–2.168 Å) as well as other NHC–metal alkyl complexes.^{3b,17} **5** also exhibits a long Cr–Cr distance of 3.1147(10) Å and an effective magnetic moment of 3.6(1) μ_B per Cr, reaffirming the Cr(III) oxidation state.

Turning to more potent alkylating reagents such as LiR or RMgX ($R = \text{Me}, \text{CH}_2\text{SiMe}_3, \text{Ph}, \text{Tolyl}, \text{CH}_2\text{CMe}_3, X = \text{Cl}, \text{Br}$) in order to fully alkylate **3** resulted in the formation of brown solutions, from which pure products could not be isolated. In one instance however, we were able to collect crystalline material resulting from an alkylation with LiMe (Scheme 4). The resulting crystal structure (see Supporting Information) has one bis-carbene ligand, with each of the NHC imidazoles coordinated to different Cr(II) centers. One bridging methyl and three terminal methyls round out the coordination spheres of the chromium ions. Furthermore, a proton on the methylene bridge between the NHC imidazoles has been removed, leaving a THF-solvated Li^+ ion to balance the anionic complex. This deprotonated methylene bridge also serves to round out the coordination spheres of the chromium ions. The very short Cr–Cr distance of 1.897 Å is excellent evidence that the product from the alkylation is indeed Cr(II).¹⁶ We believe that all the alkylations with LiR or RMgX could result in similar bimetallic Cr(II) complexes with deprotonated ligands.

To eliminate the possibility of “reductive alkylation”,¹⁸ we opted to use chromium starting materials that already contained

(14) (a) Cotton, F. A.; Eglin, J. L.; Luck, R. L.; Son, K. A. *Inorg. Chem.* **1990**, *29*, 1802. (b) Bachmann, B.; Heck, J.; Massa, W.; Pebler, J. Z. *Anorg. Allg. Chem.* **1995**, *621*, 2061.

(15) Dyer, P. W.; Gibson, V. C.; Jeffery, J. C. *Polyhedron* **1995**, *14*, 3095.

(16) Cotton, F. A.; Wilkinson, G.; Murillo, C. A.; Bochmann, M. *Advanced Inorganic Chemistry*, 6th ed.; John Wiley and Sons: New York, 1999; p 743.

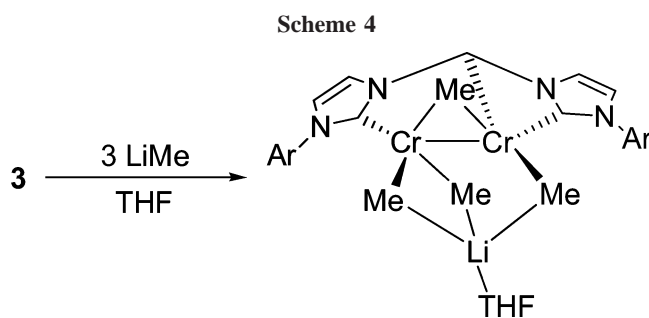
(17) (a) Simms, R. W.; Drewitt, M. J.; Baird, M. C. *Organometallics* **2002**, *21*, 2958. (b) Niehues, M.; Erker, G.; Kehr, G.; Schwab, P.; Fröhlich, R.; Blacque, O. *Organometallics* **2002**, *21*, 2905. (c) Spencer, L. P.; Winston, S.; Fryzuk, M. D. *Organometallics* **2004**, *23*, 3372. (d) Danopoulos, A. A.; Wright, J. A.; Motherwell, W. B.; Ellwood, S. *Organometallics* **2004**, *23*, 4807.

Table 3. Selected Interatomic Distances (Å) and Angles (deg) for (LCrCl)₂(μ-Cl)₃⁺BARF⁻ (**4**)

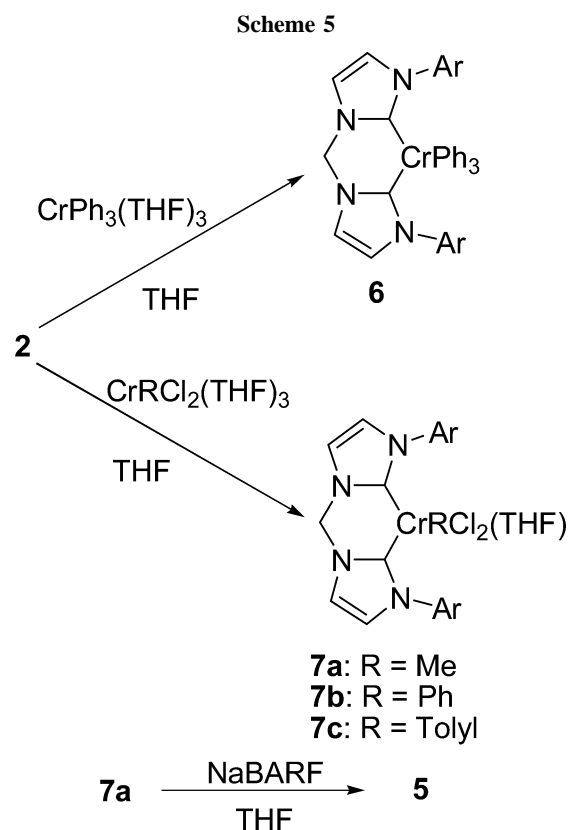
Cr(1)–C(1)	2.109(5)	Cr(2)–C(32)	2.096(5)	C(1)–Cr(1)–C(16)	85.9(2)
Cr(1)–C(16)	2.094(5)	Cr(2)–C(47)	2.108(5)	Cl(1)–Cr(1)–Cl(5)	174.23(6)
Cr(1)–Cl(1)	2.2433(16)	Cr(2)–Cl(2)	2.2419(15)	C(1)–Cr(1)–Cl(3)	172.45(14)
Cr(1)–Cl(3)	2.4042(15)	Cr(2)–Cl(3)	2.3915(14)	C(16)–Cr(1)–Cl(3)	95.22(14)
Cr(1)–Cl(4)	2.3636(15)	Cr(2)–Cl(4)	2.3702(15)	C(16)–Cr(1)–Cl(4)	172.86(15)
Cr(1)–Cl(5)	2.4039(15)	Cr(2)–Cl(5)	2.4101(15)	C(32)–Cr(1)–Cl(4)	174.35(14)

Table 4. Selected Interatomic Distances (Å) and Angles (deg) for (LCrMe)₂(μ-Cl)₃⁺BARF⁻ (**5**)

Cr(1)–C(2)	2.116(2)	Cr(2)–C(34)	2.1196(19)	C(2)–Cr(1)–C(18)	86.87(7)
Cr(1)–C(18)	2.120(2)	Cr(2)–C(50)	2.116(2)	C(1)–Cr(1)–Cl(2)	175.92(6)
Cr(1)–C(1)	2.058(2)	Cr(2)–C(33)	2.058(2)	C(18)–Cr(1)–Cl(2)	90.02(5)
Cr(1)–Cl(1)	2.3901(6)	Cr(2)–Cl(1)	2.3917(6)	C(18)–Cr(1)–Cl(3)	173.52(5)
Cr(1)–Cl(2)	2.4880(6)	Cr(2)–Cl(2)	2.3904(6)	C(2)–Cr(1)–Cl(1)	174.88(6)
Cr(1)–Cl(3)	2.3887(7)	Cr(2)–Cl(3)	2.5000(6)	C(50)–Cr(1)–Cl(1)	75.10(6)



alkyl or aryl substituents (Scheme 5). Starting with the moderately stable CrPh₃(THF)₃ in THF and exposing it to 1 equiv of the free carbene ligand immediately gave a bright green solution. Recrystallization from THF gave bright green single crystals of LCrPh₃ (**6**). The solid-state structure of **6** is shown in Figure 5. The metric data for **6** can be found in Table 5. **6** crystallizes in the orthorhombic space group *Pbcn* with a mirror plane running through C(3), C(6), C(34), and Cr. The geometry of the complex is square pyramidal with a phenyl ligand occupying the apical position; it is a rare example of five-coordinate Cr(III).^{7b,19} The most probable reason for this coordinative unsaturation is that the “folding” of the bis-carbene ligand at the bridging methylene position forces the bulky diisopropylphenyl substituents into the potential sixth coordination site of the molecule (see Figure 5). Because of this “folding” of the ligand, the apical phenyl ligand is less sterically crowded and has the shortest bond to Cr of the three aryl ligands: 2.044(4), 2.066(4), 2.079(4) Å. The Cr–carbene distances in **6** (2.228(4) and 2.244(4) Å) are considerably longer than in the previously mentioned complexes as well as in most other carbene complexes with aryl substituents, indicating the substantial amount of electron density placed on Cr by the three phenyl ligands and the carbene ligand’s inability to accept back-donation from the metal.²⁰ The effective magnetic moment for **6** at room temperature was found to be 3.7(1) μ_B, consistent with a monomeric, open-shell Cr(III) complex. Decomposition of the light-sensitive **6** over the course of a few hours under ambient light in solution or in the solid state resulted in a brown



material, from which a pure product could not be isolated. We suspect that the resulting decomposition product is a reduced, dicyclic Cr(II) compound similar to the products of the alkylation reactions mentioned above (Scheme 4).

To obtain more stable alkyl and aryl complexes, starting materials of the type CrRCl₂(THF)₃ were used to generate LCrRCl₂(THF)_n (R = Me (**7a**), Ph (**7b**), tolyl (**7c**)) (Scheme 5). These partially alkylated/arylated products were indeed much more stable than **6**; however, much like **3**, the solubility of **7a** and **7b** was very poor and only **7c** could be structurally characterized (Figure 6 and Table 6). Complex **7c** crystallizes in the monoclinic space group *P2₁/c*. The structure of **7c** shows a tolyl ligand and a chloride ligand in the plane perpendicular

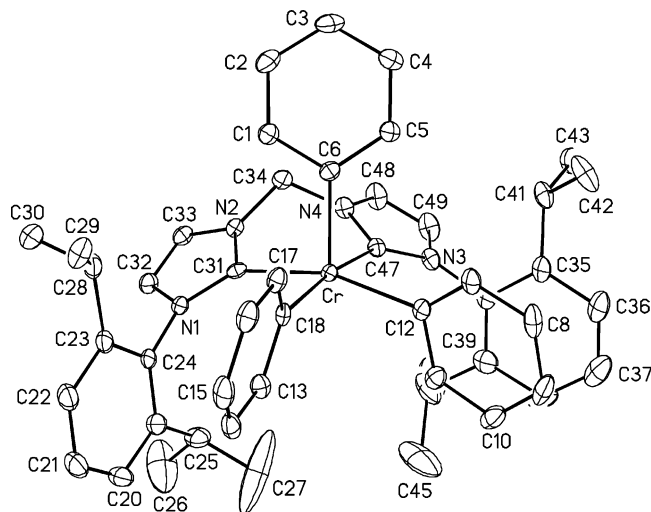
(18) (a) Bouwkamp, M. W.; Lobkovsky, E.; Chirik, P. J. *J. Am. Chem. Soc.* **2005**, *127*, 9660. (b) Humphries, M. J.; Tellmann, K. P.; Gibson, V. C.; White, A. J. P.; Williams, D. J. *Organometallics* **2005**, *24*, 2039.

(19) (a) Caddick, S.; Cloke, F. G. N.; Hitchcock, P. B.; Leonard, J.; Lewis, A. K. de K.; McKeircher, D.; Titcomb, L. R. *Organometallics* **2001**, *21*, 4318. (b) McGuinness, D. S.; Cavell, K. J.; Skelton, B. W.; White, A. H. *Organometallics* **1999**, *18*, 1596. (c) Dinger, M. B.; Mol, J. C. *Eur. J. Inorg. Chem.* **2003**, 2827. (d) Marshall, W. J.; Grushin, V. V. *Organometallics* **2003**, *22*, 1591. (e) Niemeyer, M. Z. *Anorg. Allg. Chem.* **2003**, 629, 1535. (f) Lewis, A. K. de K.; Caddick, S.; Cloke, F. G. N.; Billingham, N. C.; Hitchcock, P. B.; Leonard, J. *J. Am. Chem. Soc.* **2003**, *125*, 10066.

(20) (a) Heintz, R. A.; Leelasubcharoen, S.; Liable-Sands, L. M.; Rheingold, A. L.; Theopold, K. H. *Organometallics* **1998**, *17*, 5477. (b) Liang, Y.; Yap, G. P. A.; Rheingold, A. L.; Theopold, K. H. *Organometallics* **1996**, *15*, 5284. (c) Fryzuk, M. D.; Leznoff, D. B.; Rettig, S. J. *Organometallics* **1997**, *16*, 5116. (d) Greene, P. T.; Russ, B. J.; Wood, J. S. *J. Chem. Soc. A* **1971**, 3636. (e) Müller, E.; Krause, J.; Schmiedeknecht, K. *J. Organomet. Chem.* **1972**, *44*, 127. (f) Cotton, F. A.; Czuchajowska, J.; Falvello, L. R.; Feng, X. *Inorg. Chim. Acta* **1990**, *172*, 135.

Table 5. Selected Interatomic Distances (Å) and Angles (deg) for LCrPh₃ (**6**)

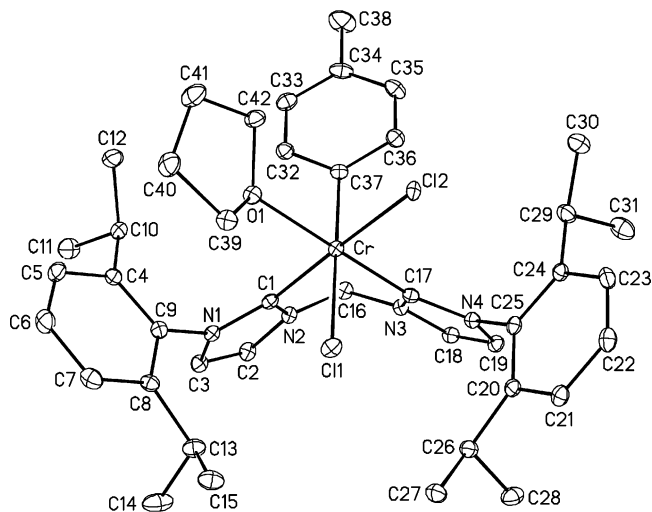
Cr–C(31)	2.228(4)	Cr–C(18)	2.079(4)	C(18)–Cr–C(12)	84.50(14)
Cr–C(47)	2.244(4)	C(31)–Cr–C(47)	83.91(14)	C(6)–Cr–C(31)	97.71(14)
Cr–C(6)	2.044(4)	C(31)–Cr–C(12)	159.94(15)	C(6)–Cr–C(47)	91.28(15)
Cr–C(12)	2.066(4)	C(47)–Cr–C(18)	171.79(15)	C(6)–Cr–C(12)	102.16(16)

**Figure 5.** ORTEP plot of LCrPh₃ (**6**) at the 30% probability level. Hydrogen atoms have been omitted for clarity.

to the bis-carbene ligand. A second chloride ligand and a coordinated THF complete the octahedral coordination sphere. The Cr–aryl bond length (2.092 Å) is longer than both the Cr–aryl bond lengths in **6** and the Cr–Me bond lengths in **5**. The Cr–carbene bond lengths of 2.128(3) and 2.151(3) Å are not nearly as long as those in **6**, but are still slightly longer than in the trichloride complex **3**. The coordinated THF has a 2.1734(19) Å bond distance from Cr, longer than the average of the two molecules in **3** (2.143(3) Å). Cl(1), *trans* to the aryl ligand in **7c**, has the shortest Cr–Cl bond length of the two chloride ligands (2.3501(8), 2.4107(7) Å).

To learn more about the true identity of **7a**, in lieu of a crystal structure determination, we attempted chloride abstraction from **7a** in the hope that a chloride ligand would be labile enough to remove, as was in the case of complex **3**. However, like complex **3**, the resulting chloride abstraction product was not mononuclear, but turned out to be the BARF[−] complex of **5** (Scheme 5). Also similar to **3**, complexes **7b** and **7c** exhibit a color change to green when exposed to vacuum or washed with Et₂O. This would suggest that the coordinated THF in **7b** and **7c** is also quite labile. Thus, it would appear that the normally octahedral geometry of Cr(III) can be altered to what would most likely be a square pyramidal geometry, much like **6**, with this strongly donating bis-carbene ligand. In the case of **7a**, we believe that the complex does not coordinate THF at all. There is no color change when exposing the complex to vacuum or when washing it with Et₂O. The lower solubility of the complex when compared to **7b** and **7c** as well as **3** would also suggest the absence of a THF ligand.

Complexes of Cr(II) were also prepared in order to determine if a correlation between oxidation state and catalyst activity existed. Thus, the bis-carbene ligand was coordinated to Cr(II) by addition of the free carbene ligand to CrCl₂ in THF, giving a bright blue insoluble product, tentatively assigned as LCrCl₂-(THF) (**8a**) on the basis of its reactivity and synthesis via another route (*vide infra*). The effective magnetic moment for **8a** was found to be 4.9(1) μ_B, which is consistent with a Cr(II), d⁴ system. Because of the inability to structurally characterize **8a**

**Figure 6.** ORTEP plot of LCrCl₂(Tol)(THF) (**7c**) at the 30% probability level. Hydrogen atoms have been omitted for clarity.

due to its very poor solubility, the bromide analogue, **8b**, was synthesized (Scheme 6). Addition of the bis-imidazolium dibromide salt (**1**) to a THF solution of Cr[N(SiMe₃)₂]₂ resulted in a bright blue solution, from which blue crystals of **8b** grew at −30 °C. The molecular structure of **8b** can be found in Figure 7, and the corresponding metric data are in Table 7. **8b** crystallizes in the monoclinic space group *P*2₁/*c*. The Cr(II) ion exists in a square pyramidal geometry similar to **6**, having a bromide ligand, Br(1), and a THF ligand in the plane of the chelating NHC ligand and a second bromide ligand, Br(2), perpendicular to the plane of the NHC, bromide, and THF ligands. While the in-plane Br(1)–Cr bond distance is 2.5277(12) Å and is on par with most Cr–Br distances in the literature (av = 2.542 Å),¹¹ the perpendicular Br(2)–Cr bond distance is much longer at 2.6800(12) Å. Also, the chromium carbene distances of 2.162(7) and 2.173(7) Å are longer than all the aforementioned complexes, with the exception of the triphenyl complex **6**. Like **8a**, complex **8b** shows an effective magnetic moment that is consistent with four unpaired electrons; μ_{eff} = 4.7(1) μ_B. Halide exchange to convert **8b** to **8a** was attempted in order to demonstrate the similarity of **8a** and **8b**. Thus, **8b** was dissolved in THF and treated with excess NEt₄Cl. Stirring for 2 h resulted in the precipitation of a blue powder. An IR spectrum of this blue precipitate was indistinguishable from an authentic IR spectrum of **8a**.

Polymerization Experiments. It is well documented that coordinative unsaturation is a necessary condition for ethylene polymerization.²¹ Thus, complexes **3–5** and **7a–c** showed no ability to polymerize ethylene by themselves, regardless of conditions. The existence of a metal–carbon bond has also been shown to be essential for catalytic ethylene polymerization.²¹ However, none of the complexes that contained chromium–carbon bonds (**5**, **6**, and **7a–c**) exhibited any ability to polymerize ethylene without a cocatalyst. Even square pyramidal **6**, which essentially meets both requirements, did not polymerize ethylene even with the Lewis acid B(C₆F₅)₃ or the strong acid

(21) Theopold, K. H. *Eur. J. Inorg. Chem.* **1998**, 15.

Table 6. Selected Interatomic Distances (Å) and Angles (deg) for $\text{LCrCl}_2(\text{Tol})$ (**7c**)

Cr–C(1)	2.151(3)	Cr–O(1)	2.1734(19)	C(17)–Cr–O(1)	176.68(9)
Cr–C(17)	2.128(3)	C(1)–Cr–Cl(1)	85.74(7)	C(17)–Cr–Cl(1)	88.69(7)
Cr–C(37)	2.092(3)	C(1)–Cr–Cl(2)	175.32(7)	C(17)–Cr–Cl(2)	95.95(7)
Cr–Cl(1)	2.3501(8)	C(1)–Cr–C(37)	91.22(10)	C(17)–Cr–C(37)	88.81(10)
Cr–Cl(2)	2.4107(7)	C(1)–Cr–O(1)	92.85(9)	C(37)–Cr–Cl(1)	176.20(7)

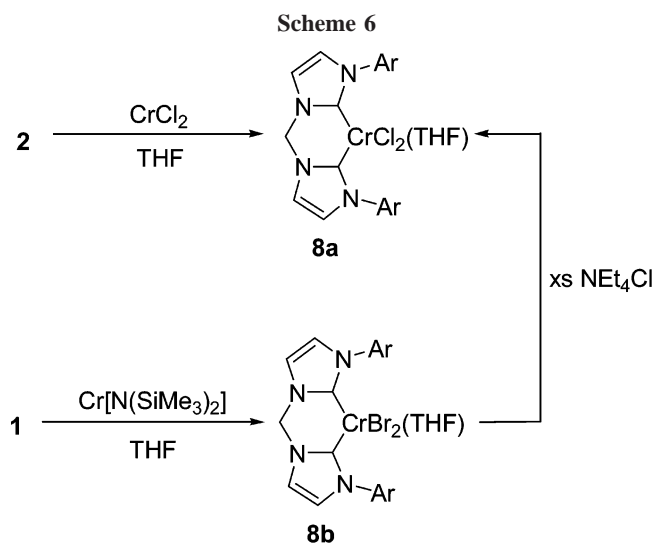
Table 7. Selected Interatomic Distances (Å) and Angles (deg) for $\text{LCrBr}_2(\text{THF})$ (**8b**)

Cr–C(1)	2.162(7)	Cr–O(1)	2.121(4)	C(1)–Cr–O(1)	167.7(2)
Cr–C(17)	2.173(6)	C(1)–Cr–C(17)	86.5(2)	C(17)–Cr–Br(1)	165.26(16)
Cr–Br(1)	2.5277(12)	C(1)–Cr–Br(1)	94.66(17)	C(17)–Cr–Br(2)	91.28(15)
Cr–Br(2)	2.6800(12)	C(1)–Cr–Br(2)	99.57(17)	Br(1)–Cr–Br(2)	102.99(4)

Table 8. Ethylene Polymerization Results for Complexes **3–6** and **7a–c**^a

catalyst	[Cr], mM	yield, g	activity ^b
3 , Et ₂ AlCl	1.43	0.553	1871
3 , MAO	1.43	0.094	318
4 , MAO	0.77	0.241	1513
5 , MAO	0.73	0.260	1722
6 , MAO	1.46	trace amount	0
7a , MAO	1.48	0.198	647
7b , MAO	1.46	0.111	363
7c , MAO	1.47	0.099	325
8a or 8b , MAO	1.44	0	0

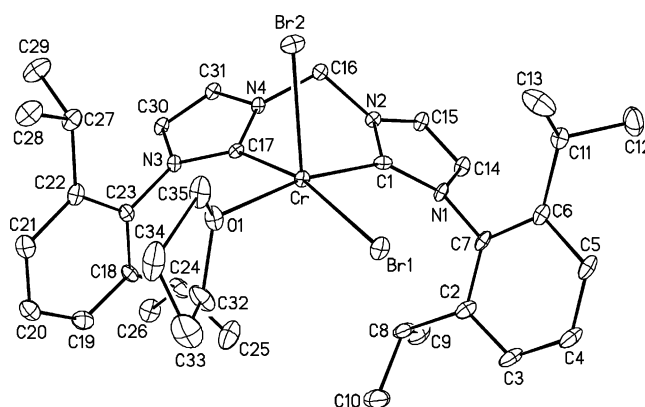
^a See the Experimental Section for details. ^b g(product) mol(Cr)⁻¹ bar⁻¹ h⁻¹.



H^+BARF^- present as cocatalyst. With the proper cocatalyst (MAO or Et₂AlCl), however, complexes **3–6** and **7a–c** were able to polymerize ethylene. The results of these experiments are listed in Table 8.

Polymerization reactions with **3** gave moderate amounts of polymer, which were analyzed in order to obtain a general idea of the type of polymer produced by these bis-carbene complexes. With either MAO or Et₂AlCl as cocatalyst, **3** produced polymer with no apparent branching and polydispersities of 27.3 for the Et₂AlCl-cocatalyzed reaction and 25.5 for the MAO-cocatalyzed reaction. Complex **3** also showed signs of multisite catalysis, and at this point, we do not wish to infer what the structure of these catalysts may be.

From the activities and polymer yields of complexes **3**, **7b**, and **7c**, it may be possible that the structures of the three complexes in their catalytically active state are similar, even though **7b** and **7c** have metal–carbon bonds and **3** does not.

**Figure 7.** ORTEP plot of $\text{LCrBr}_2(\text{THF})$ (**8b**) at the 30% probability level. Hydrogen atoms have been omitted for clarity.

However, the metal–aryl bonds of **7b** and **7c** may be quite strong and unable to insert ethylene, as can be seen from the poor catalytic activity of **6** and the slightly more active **7a**, which contains a weaker Cr–CH₃ bond.²² It is, however, slightly unusual that the binuclear complexes **4** and **5** are much more active than the monomeric complexes. One reason for this may be the increased Lewis acidity caused by the cationic nature of the complex, but a binuclear polymerization mechanism cannot be ruled out. On the other hand, the Cr(II) halide complexes **8a** and **8b** were inactive to ethylene when exposed to MAO, thus showing that the more Lewis acidic Cr(III) is superior for ethylene polymerization within this system.

Conclusion

We have prepared and structurally characterized several bis-carbene Cr(III) complexes. These complexes catalyze the polymerization of ethylene with a MAO cocatalyst, but the activities are low and the polymers have a broad molecular weight distribution. The organometallic chemistry of chromium supported by this bis-carbene ligand is impacted by the ease with which the complexes of Cr(III) are reduced to Cr(II). This can be attributed to the very strong σ -donating, but soft character of the carbene ligand and its affinity for the softer Cr(II) rather than the hard Cr(III). Thus, this ligand system may be better suited for lower valent chromium chemistry. However, as can be seen from the last entry in Table 8, the Cr(II) halide complexes **8a** and **8b** do not polymerize ethylene even when activated by MAO or alkylaluminum reagents. With this piece of evidence in hand, it seems that dropping to lower valencies of chromium would not be a successful strategy for studying

(22) Crabtree, R. H. *The Organometallic Chemistry of the Transition Metals*, 3rd ed.; John Wiley and Sons: New York, 2001; p 55.

ethylene polymerization by NHC-supported organochromium complexes. Therefore, we plan to divert our efforts to more fruitful avenues of research in our studies of organochromium-mediated ethylene polymerization.

Experimental Section

General Considerations. All manipulations were carried out with standard Schlenk, vacuum line, and glovebox techniques. Pentane, diethyl ether, tetrahydrofuran, and toluene were distilled from purple Na benzophenone/ketyl solutions. THF-*d*₈ was predried over potassium and stored under vacuum over Na/K. CD₂Cl₂ was predried with P₂O₅ and stored under vacuum over 4 Å molecular sieves. CrCl₃ (anhydrous) and CrCl₂ (anhydrous) were purchased from Strem Chemical Co. ((Trimethylsilyl)methyl)lithium was purchased as a 1 M solution in pentane from Aldrich, crystallized from solution at -30 °C, and isolated as a white crystalline solid. Methylolithium, trimethylaluminum, phenylmagnesium chloride, dibromomethane, and potassium hexamethyldisilazane were purchased from Aldrich and used as received. 3-Di-2,6-diisopropylphenylimidazole,²³ CrCl₃(THF)₃,²⁴ CrPh₃(THF)₃,²⁵ sodium tetra-3,5-di-trifluoromethylphenyl borate,²⁶ CrMeCl₂(THF)₃,²⁷ CrPhCl₂(THF)₃,²⁸ Cr(Tolyl)Cl₂(THF)₃,²⁹ and Cr[N(SiMe₃)₂]₂³⁰ were prepared according to literature procedures. NMR spectra were taken on a Bruker AM-250 spectrometer and were referenced to the residual protons of the solvent (DMSO-*d*₆, 3.70 ppm; THF-*d*₈, 1.73 and 3.58 ppm; CD₂Cl₂, 5.32 ppm).³¹ FTIR spectra were taken on a Mattson Alpha Centauri spectrometer with a resolution of 4 cm⁻¹. UV/vis spectra were taken on a Hewlett-Packard 8453 spectrophotometer. Mass spectra were obtained by the University of Delaware Mass Spectrometry Facility. Elemental analyses were performed by Desert Analysis.³² Room-temperature magnetic susceptibility measurements were carried out using a Johnson Matthey magnetic susceptibility balance.

Preparation of 1,1'-Methylene-3,3'-di-2,6-diisopropylphenylimidazolium Dibromide (1). 3-Di-2,6-diisopropylphenylimidazole (17.14 g, 75.2 mmol) and 2.65 mL (37.8 mmol) of CH₂Br₂ in 250 mL of xylene were added to an ampule. The solution was degassed and heated to 200 °C for 3 days. The white precipitate of **1** that formed was collected by filtration and washed with hexanes to give 16.16 g (68%). **1** can be recrystallized by slow evaporation of a DMSO solution of the compound. ¹H NMR (DMSO-*d*₆): δ 10.57 (2H, s, CH(imid)), 8.89 (2H, s, CH(imid)), 8.47 (2H, s, CH(imid)), 7.83 (2H, t, CH(aromatic)), *J*_{HH} = 7.2 Hz), 7.67 (4H, d, CH(aromatic)), *J*_{HH} = 10.8 Hz), 7.31 (2H, s, CH₂), 2.46 (4H, m,

CH(i-Pr), *J*_{HH} = 7.2 Hz), 1.31 (24H, d, CH₃(i-Pr), *J*_{HH} = 3.6 Hz) ppm. ¹³C NMR (DMSO-*d*₆): δ 144.90 (CH(imid)), 139.11 (CH(imid)), 131.86 (CH(aromatic)), 130.11 (CH(aromatic)), 125.79 (CH(aromatic)), 124.64 (CH(aromatic)), 123.25 (CH(aromatic)), 58.69 (CH₂), 28.03 (CH(i-Pr)), 23.82 (CH₃(i-Pr)) ppm. IR (KBr; cm⁻¹): 3076 (w), 3012 (w), 2959 (s), 2869 (m), 1530 (m), 1483 (m), 1181 (s), 1063 (w), 808 (m), 758 (m). Anal. Calcd for C₃₁H₄₂Br₂N₄·3H₂O: C, 54.47; H, 6.93; N, 8.20. Found: C, 54.83; H, 7.12; N, 8.28. MS (*m/z* (%)): 469 (95) [M⁺ - 2Br]. Mp: >300 °C.

Preparation of 1,1'-Methylene-3,3'-di-2,6-diisopropylphenylimidazole-2,2'-diylidene (2). To a slurry of **1** (1.018 g, 2.17 mmol) in 75 mL of THF at RT was slowly added 0.745 g (4.35 mmol) of solid K[N(SiMe₃)₂]. The resulting green solution was allowed to stir at RT overnight, over which time it turned brown. The THF was then stripped from the brown solution, and the residue was extracted into THF and filtered through Celite. The filtrate was concentrated and cooled to -30 °C overnight. The purified product was filtered and washed with cold pentane to give **2** as a white powder in two crops in 69% yield (0.518 g). ¹H NMR (CD₂Cl₂): δ 7.32 (2H, t, CH(aromatic)), *J*_{HH} = 7.2 Hz), 7.21 (4H, d, CH(aromatic)), *J*_{HH} = 10.1 Hz), 7.19 (2H, s, CH₂), 6.49 (2H, s, CH(imid)), 6.29 (2H, s, CH(imid)), 2.81 (4H, m, CH(i-Pr), *J*_{HH} = 6.8 Hz), 1.30 (12H, d, CH₃(i-Pr), *J*_{HH} = 6.8 Hz), 1.14 (12H, d, CH₃(i-Pr), *J*_{HH} = 7.2 Hz) ppm. ¹³C NMR (CD₂Cl₂): δ 219.01 (C(imid)), 146.30 (CH(imid)), 138.86 (CH(imid)), 129.07 (CH(aromatic)), 123.74 (CH(aromatic)), 122.89 (CH(aromatic)), 118.16 (CH(aromatic)), 65.72 (CH₂), 28.61 (CH(i-Pr)), 23.86 (CH₃(i-Pr)) ppm. IR (KBr; cm⁻¹): 3139 (w), 3066 (w), 2961 (s), 2866 (m), 1472 (s), 1361 (s), 1312 (m), 1247 (m), 1231 (m), 1060 (w), 940 (w), 804 (w), 761 (m). MS for ¹²C_{30¹H₃₈¹⁴N₄ [M⁺ - CH₃]: calcd, 454.30965; found, 454.30924. Mp: 121 °C dec.}

Preparation of (1,1'-Methylene-3,3'-di-2,6-diisopropylphenylimidazole-2,2'-diylidene)trichlorotetrahydrofuranchromium(III), LCrCl₃(THF) (3). To a slurry of 0.141 g (0.377 mmol) of CrCl₃(THF)₃ in 15 mL of THF was added 0.175 g (0.374 mmol) of **2**. The resulting solution was allowed to stir at room temperature overnight, over which time a blue precipitate formed. The solid was collected and washed with THF to give 0.263 g of **3** (89%). X-ray-quality crystals of **3** were grown by very slow cooling of a hot THF solution of the complex. ¹H NMR (THF-*d*₆): δ 8.70 (br, 12H), 7.12 (br, 12H) ppm. IR (KBr; cm⁻¹): 3130 (w), 3096 (w), 2962 (s), 2931 (s), 2866 (m), 1459 (s), 1409 (m), 1353 (m), 1273 (m), 1185 (m), 1116 (w), 1061 (m), 1017 (w), 861 (m), 789 (m), 760 (m). Anal. Calcd for C₃₅H₄₈N₄O₄CrCl₃: C, 60.15; H, 6.89; N, 8.02. Found: C, 59.11; H, 7.28; N, 8.00. MS (*m/z* (%)): 684 (15) [M⁺ - CH₃], 610 (17) [M⁺ - THF, CH₃]. UV/vis (THF; λ_{max}, nm (ε, M⁻¹ cm⁻¹)): 480 (81), 635 (152). μ_{eff} (294 K) = 4.0(1) μ_B. Mp: 228 °C dec.

Preparation of Bis(1,1'-methylene-3,3'-di-2,6-diisopropylphenylimidazole-2,2'-diylidene)pentachlorodichromium(III) Tetrakis(3,5-di-trifluoromethylphenyl)borate, [(LCrCl₂(μ-Cl)₃]BARF (4). To a green slurry of **3** (0.054 g, 0.08 mmol) in 10 mL of Et₂O was added 0.068 g of NaBARF (0.08 mmol). The green solution was allowed to stir at room temperature for 3 h. The solvent was then removed in vacuo and the residue extracted with Et₂O. The solution was filtered to remove NaCl, then concentrated and cooled to -30 °C overnight to give colorless crystals of NaBARF, which were removed by filtration. The filtrate was then concentrated and cooled overnight to give green crystals of **4** in 74% yield (0.064 g). ¹H NMR (CD₂Cl₂): δ 9.79 (vb, 4H), 7.76 (BARF, 8H), 7.59 (BARF, 4H) ppm. IR (KBr; cm⁻¹): 3096 (w), 2964 (m), 2933 (m), 2871 (w), 1465 (m), 1397 (m), 1355 (s), 1284 (s), 1125 (s), 1062 (m), 887 (m), 682 (m). Anal. Calcd for C₉₄H₉₂N₈Cr₂Cl₅BF₂₄: C, 54.24; H, 4.43; N, 5.38. Found: C, 53.61; H, 4.50; N, 5.20. MS (*m/z* (%)): 650 (60), 631 (18), 437 (53), 388 (98). UV/vis (Et₂O; λ_{max}, nm (ε, M⁻¹ cm⁻¹)): 460 (315), 629 (163). μ_{eff}(294 K) = 3.6-(1) μ_B per Cr. Mp: 232 °C dec.

(23) (a) Shin, K. H. U.S. Patent 4,636,574, 1987. (b) Johnson, A. L. U.S. Patent 3,637,731, 1972.

(24) Herwig, W.; Zeiss, H. H. *J. Org. Chem.* **1958**, *9*, 1404.

(25) Herwig, W.; Zeiss, H. H. *J. Am. Chem. Soc.* **1957**, *79*, 6561.

(26) Bahr, S. R.; Boudjouk, P. *J. Org. Chem.* **1992**, *57*, 5545.

(27) Nishimura, K.; Kuribayashi, H.; Yamamoto, A.; Ikeda, S. *J. Organomet. Chem.* **1972**, *37*, 317.

(28) Hein, F.; Schmiedeknecht, K. *Z. Anorg. Allg. Chem.* **1967**, *352*, 138.

(29) Daly, J. J.; Sneed, R. P. A.; Zeiss, H. H. *J. Am. Chem. Soc.* **1966**, *88*, 4287.

(30) Bradley, D. C.; Hursthouse, M. B.; Newing, C. W.; Welch, A. J. *Chem. Commun.* **1972**, 219.

(31) Many complexes were very insoluble, making most solution characterization difficult. ¹H NMR spectra were collected with a very high number of scans, still resulting in poor resolution, and thus integrations are highly uncertain. UV/vis spectra for complexes **7a** and **8a** were not recorded because of solubility issues as well.

(32) Elemental analyses for **3**, **7c**, and **8b** are low in content for carbon and hydrogen. The ease with which THF is lost for the complexes makes it difficult to quantify the amount of solvent lost prior to sample submission. The air sensitivity of these complexes may also give rise to the poor elemental analysis as well. The poor solubility of complexes **7a**, **7b**, and **8a** made purification of the complexes difficult; thus elemental analyses of these complexes were not attempted. Additionally, the extreme air, temperature, and light sensitivity of **6** made elemental analysis of the sample impossible.

Table 9. Crystallographic Data for 1, 3–6, 7c, and 8b

	1	3	4	5	6	7c	8b
formula	C ₃₁ H ₄₁ Br ₂ N ₄ ·3H ₂ O	C ₃₅ H ₄₈ Cl ₃ CrN ₄ O·2.5C ₄ H ₈ O	C ₁₀₀ H ₉₅ BCl ₅ ·Cr ₂ F ₂₄ N ₈ ·2.5C ₄ H ₁₀ O	C ₁₀₂ H ₁₀₁ BCl ₃ ·Cr ₂ F ₂₄ N ₈ ·5.5C ₄ H ₁₀ O	C ₅₂ H ₅₈ CrN ₄ ·2.5C ₄ H ₈ O	C ₄₃ H ₅₇ Cl ₂ ·CrN ₄ O·2CH ₂ Cl ₂	C ₃₅ H ₄₈ CrBrN ₄ O·4C ₄ H ₈ O
fw	683.55	879.38	2342.20	2579.83	971.28	1009.58	1041.01
space group	<i>Pbcn</i>	<i>P</i> $\bar{1}$	<i>P</i> $\bar{1}$	<i>P</i> $\bar{1}$	<i>Pbcn</i>	<i>P2</i> ₁ / <i>c</i>	<i>P2</i> ₁ / <i>c</i>
color	colorless	blue	green	red	green	maroon	blue
<i>a</i> , Å	15.222(2)	13.8591(14)	16.948(3)	18.305(4)	21.823(3)	15.137(3)	13.350(3)
<i>b</i> , Å	21.681(3)	16.0822(17)	17.769(3)	19.122(4)	17.743(2)	20.501(3)	25.522(6)
<i>c</i> , Å	10.5130(16)	21.096(2)	21.691(4)	21.462(4)	28.131(3)	16.090(3)	15.668(4)
α , deg	90	92.015(2)	106.082(3)	97.118(3)	90	90	90
β , deg	90	92.343(3)	106.082(3)	107.807(3)	90	93.218(3)	102.062(4)
γ , deg	90	101.366(2)	101.000(4)	106.509(3)	90	90	90
<i>V</i> , Å ³	3469.6(9)	4601.3(8)	5771.9(18)	6672(2)	10892(2)	4985.6(14)	5220(2)
<i>Z</i> , <i>Z'</i>	4, 1	4, 2	2, 1	2, 1	8, 1	4, 1	4, 1
<i>D</i> (calcd), g cm ⁻³	1.309	1.269	1.348	1.284	1.185	1.345	1.325
μ (Mo K α), mm ⁻¹	2.370	0.466	0.394	0.310	0.257	0.696	1.797
temp, K	120	120	120	120	100	120	120
no. data/params	4034/198	14 930/970	15 066/1207	29 427/1247	8543/651	11 380/541	8151/396
GOF on <i>F</i> ²	1.066	1.045	1.088	1.084	1.060	1.063	1.011
<i>R</i> (<i>F</i>), % ^a	6.94	7.98	7.25	5.76	7.69	5.66	7.07
<i>R</i> _w (<i>F</i> ²), % ^a	8.07	14.57	9.38	6.79	9.39	7.35	10.84

^a Quantity minimized: $R_w(F^2) = \sum[w(F_o^2 - F_c^2)^2]/\sum[(wF_o^2)^2]^{1/2}$; $R = \sum\Delta/\sum(F_o)$, $\Delta = |F_o - F_c|$.

Preparation of Bis(1,1'-methylene-3,3'-di-2,6-diisopropylphenylimidazole-2,2'-diylidene)trichlorodimethyldichromium(III) Tetraakis(3,5-di-trifluoromethylphenyl)borate, [(LCrMe)₂(μ -Cl)₃]-BARF (5). A 0.128 g (0.19 mmol) amount of **7a** was suspended in 15 mL of THF. To the slurry was added 0.168 g of NaBARF (0.20 mmol), which resulted in an immediate color change to red. The solution was allowed to stir for 30 min, and then the solvent was removed in vacuo. The residue was extracted with Et₂O and filtered to remove NaCl. The solution was concentrated and cooled to -30 °C overnight to yield colorless crystals of NaBARF, which were removed by filtration. Concentrating the filtrate and cooling the solution overnight gave bright red crystals of **5** in 71% yield (0.147 g). ¹H NMR (CD₂Cl₂): δ 8.98 (br, 6H), 7.76 (BARF, 8H), 7.59 (BARF, 4H), 1.47 (br, 48H), -9.31 (vb, 6H) ppm. IR (KBr; cm⁻¹): 3070 (w), 2966 (s), 2931 (s), 2869 (m), 1463 (s), 1406 (s), 1353 (s), 1280 (s), 1137 (s), 1058 (m), 887 (m), 838 (m), 756 (m), 712 (m), 682 (m), 670 (m). Anal. Calcd for C₉₆H₉₈N₈Cr₂Cl₃BF₂₄: C, 56.51; H, 4.82; N, 5.49. Found: C, 56.24; H, 4.77; N, 5.43. MS (*m/z* (%)): 590 (36) [M⁺ - CH₃, LCrMeCl, BARF], 555 (100) [M⁺ - CH₃, LCrMeCl₂, BARF]. UV/vis (Et₂O; λ_{\max} , nm (ϵ , M⁻¹ cm⁻¹)): 414 (1398), 546 (149). μ_{eff} (294 K) = 3.6(1) μ_B per Cr. Mp: 211 °C dec.

Preparation of Bis(1,1'-methylene-3,3'-di-2,6-diisopropylphenylimidazole-2,2'-diylidene)triphenylchromium(III), LCrPh₃ (6). CrPh₃(THF)₃ (0.237 g, 0.47 mmol) was dissolved in 15 mL of THF that had been chilled to -30 °C. To this red solution was added 0.222 g (0.47 mmol) of **2**, which caused the color of the solution to turn bright green. The THF was immediately removed in vacuo, and the residue redissolved in THF and filtered. The filtrate was concentrated and cooled to -30 °C for crystallization overnight. A 0.189 g (53%) amount of **6** was collected as bright green crystals. ¹H NMR (THF-*d*₈): δ 14.42 (vb, 6H), 8.42 (br, 6H), 1.10 (br, 24H), -12.10 (vb, 5H), -21.89 (vb, 5H) ppm. IR (KBr; cm⁻¹): 3034 (m), 2960 (vs), 2928 (s), 2866 (m), 1559 (w), 1463 (s), 1404 (m), 1360 (w), 1258 (m), 1057 (w), 802 (w), 760 (m), 724 (m), 697 (m). UV/vis (THF; λ_{\max} , nm (ϵ , M⁻¹ cm⁻¹)): 668 (420). μ_{eff} (294 K) = 3.7(1) μ_B .

Preparation of Bis(1,1'-methylene-3,3'-di-2,6-diisopropylphenylimidazole-2,2'-diylidene)dichloromethylchromium(III), LCrMeCl₂ (7a). A 0.183 g (0.52 mmol) amount of CrMeCl₂(THF)₃ was suspended in 15 mL of THF, and to this was added 0.242 g (0.52 mmol) of **2**. Stirring for 2 h resulted in a tan precipitate, which was collected by filtration and washed with THF to give 0.277 g of **7a** (79%). ¹H NMR (THF-*d*₈): δ 0.12 (br). IR (KBr; cm⁻¹):

3070 (w), 2962 (s), 2923 (m), 2867 (m), 1465 (m), 1406 (w), 1376 (m), 1351 (w), 1263 (w), 1185 (w), 1113 (w), 1060 (w), 802 (w), 756 (m). MS (*m/z* (%)): 514 (20), 403 (27), 186 (100). μ_{eff} (294 K) = 3.8(1) μ_B . Mp: 202 °C dec.

Preparation of Bis(1,1'-methylene-3,3'-di-2,6-diisopropylphenylimidazole-2,2'-diylidene)dichlorophenylchromium(III) Tetrahydrofuran, LCrPhCl₂(THF) (7b). A 0.344 g (0.83 mmol) amount of CrPhCl₂(THF)₃ was suspended in 40 mL of THF, and to it was added 0.384 g (0.82 mmol) of **2**. Stirring for 3 h resulted in a brown-red solution, which was concentrated and cooled to -30 °C overnight, yielding **7b** (0.475 g, 78%) as a pale pink solid. ¹H NMR (THF-*d*₈): δ 8.79 (vb, 2H), 7.04 (br, 6H), 1.21 (br, 12H), 0.10 (br, 2H). IR (KBr; cm⁻¹): 3087 (m), 2962 (s), 2925 (m), 2866 (s), 1465 (s), 1408 (s), 1379 (m), 1352 (m), 1264 (m), 1184 (m), 1112 (w), 1059 (m), 803 (m), 759 (s). MS (*m/z* (%)): 403 (11), 186 (27). UV/vis (THF; λ_{\max} , nm (ϵ , M⁻¹ cm⁻¹)): 368 (519), 429 (172). μ_{eff} (294 K) = 4.0(1) μ_B . Mp: 189 °C dec.

Preparation of Bis(1,1'-methylene-3,3'-di-2,6-diisopropylphenylimidazole-2,2'-diylidene)dichlorotolylchromium(III) Tetrahydrofuran, LCr(Tolyl)Cl₂(THF) (7c). A 0.164 g amount (0.38 mmol) of Cr(Tolyl)Cl₂(THF)₃ was suspended in 20 mL of THF, and to it was added 0.178 g (0.38 mmol) of **2**. Stirring for 3 h resulted in a brown-red solution, which was concentrated and cooled to -30 °C overnight, yielding **7c** (0.204 g, 71%) as a pale pink solid. X-ray-quality crystals were grown from a THF/CH₂Cl₂ solution of the complex. ¹H NMR (THF-*d*₈): δ 8.78 (vb, 2H), 7.26 (br, 6H), 1.12 (br, 12H). IR (KBr; cm⁻¹): 3077 (m), 2961 (s), 2928 (s), 2867 (s), 1590 (w), 1563 (w), 1462 (s), 1405 (m), 1382 (m), 1352 (m), 1260 (m), 1182 (m), 1105 (m), 1060 (m), 802 (m), 759 (s). Anal. Calcd for C₄₂H₅₅N₄CrCl₂O: C, 66.82; H, 7.34; N, 7.42. Found: C, 58.43; H, 5.82; N, 7.95. MS (*m/z* (%)): 403 (13), 186 (43). UV/vis (THF; λ_{\max} , nm (ϵ , M⁻¹ cm⁻¹)): 372 (478), 444 (332). μ_{eff} (294 K) = 3.6(1) μ_B . Mp: 192 °C dec.

Preparation of Bis(1,1'-methylene-3,3'-di-2,6-diisopropylphenylimidazole-2,2'-diylidene)dichlorochromium(II) Tetrahydrofuran, LCrCl₂(THF) (8a). To a slurry of 0.188 g (1.53 mmol) of CrCl₂ in 30 mL of THF was added 0.719 g (1.53 mmol) of **2**. Stirring overnight at room temperature produced a bright blue precipitate, which was collected by filtration and washed with THF to give 0.816 g (90%) of **8a**. IR (KBr; cm⁻¹): 3080 (m), 2963 (s), 2910 (s), 2866 (s), 1593 (w), 1559 (w), 1466 (s), 1404 (s), 1362 (m), 1265 (m), 1184 (m), 1106 (m), 1059 (m), 958 (w), 804 (s), 757 (s). MS (*m/z* (%)): 560 (7), 514 (100). μ_{eff} (294 K) = 4.9(1) μ_B . Mp: 147 °C dec.

Preparation of Bis(1,1'-methylene-3,3'-di-2,6-diisopropylphenylimidazole-2,2'-diylidene)dibromochromium(II) Tetrahydrofuran, $\text{LCrBr}_2(\text{THF})$ (8b**).** $\text{Cr}[\text{N}(\text{SiMe}_3)_2]_2$ (0.186 g, 0.36 mmol) was dissolved in 20 mL of THF. A 0.227 g (0.36 mmol) amount of **1** was then added, producing a green solution. The solution was allowed to react at room temperature overnight, then cooled to -30 °C for 3 h to give blue crystals of **8b** in 79% yield (0.214 g). ^1H NMR ($\text{THF}-d_8$): δ 9.57 (br, 6H), 6.71 (br, 4H), 2.57 (br, 24H), -16.12 (vb, 2H). IR (KBr; cm^{-1}): 3082 (m), 2966 (s), 2907 (s), 2866 (s), 1592 (w), 1556 (w), 1540 (m), 1462 (s), 1403 (m), 1384 (m), 1256 (w), 1187 (s), 1117 (w), 1061 (m), 935 (w), 804 (s), 757 (s). Anal. Calcd for $\text{C}_{35}\text{H}_{48}\text{N}_4\text{OCrBr}_2$: C, 55.86; H, 6.40; N, 7.45. Found: C, 53.81; H, 6.37; N, 7.39. MS (m/z (%)): 650 (42), 631 (16), 437 (60), 388 (100). UV/vis (THF; λ_{max} , nm (ϵ , $\text{M}^{-1} \text{cm}^{-1}$): 379 (1658), 719 (314). $\mu_{\text{eff}}(294 \text{ K}) = 4.7(1) \mu_{\text{B}}$. Mp: 162 °C dec.

Crystallographic Structure Determinations. A summary of crystal data collection and refinement parameters for compounds **1**, **3–6**, **7c**, and **8b** can be found in Table 9. Suitable crystals were selected, mounted with viscous oil, and cooled to the data collection temperature. Data were collected on a Bruker APEX CCD diffractometer using graphite-monochromated Mo $K\alpha$ radiation ($\lambda = 0.71073$). Unit cell parameters were obtained from three sets of 20 frames using 0.3° scans from different sections of the Ewald sphere. Data sets were corrected for absorption using SADABS multiscan methods.³³ No symmetry higher than triclinic was observed for complexes **3–5**. Systematic absences in the diffraction data and unit cell parameters are consistent for *Pbcn* for compounds **1** and **6** and *P2₁/c* for complexes **7c** and **8b**. In all the structures, the centrosymmetric space group option yielded chemically reasonable and computationally stable results of refinement. Structures were solved using direct methods and refined with full-matrix least-squares methods based on F^2 . The structure of **1** is located on a 2-fold rotation axis. Two symmetry unique but chemically similar

molecules of **3** are located in the asymmetric unit. Complex **5** shows several disordered CF_3 groups in the BARF anion. Several structures display cocrystallized solvent molecules: **1** has 3 H_2O molecules in the asymmetric unit, **3** has 5 THF molecules in the asymmetric unit, **4** has 1 THF, 1 toluene, and 1.5 Et_2O molecules cocrystallized in the asymmetric unit, **5** displays 5.5 THF molecules and 1 pentane molecule in the asymmetric unit, **6** has 2.5 THF molecules and 1 benzene molecule per asymmetric unit, **7c** has 3 CH_2Cl_2 molecules per asymmetric unit, and **8b** displays 4 severely disordered THF molecules per asymmetric unit. Solvent molecules for **4**, **5**, and **8b** have been modeled as diffuse contributions.³⁴ All non-hydrogen atoms were refined anisotropically. All hydrogen atoms were treated as idealized contributions. All structure factors are included in the SHELXTL program library.³³ Details of crystal structure data are available from the Cambridge Structural Database under depository numbers **1**, 607997; **3**, 607999; **4**, 607998; **5**, 608003; **6**, 608000; **7c**, 608002; and **8b**, 608001.

General Ethylene Polymerization Procedure. In a glovebox, the precatalyst (0.036–0.100 mmol) was dissolved in 30–40 g of toluene. To the precatalyst was added either MAO (10 wt % solution in toluene) or Et_2AlCl (1.0 M solution in hexanes). The mixture was placed in a sealed Parr reactor, and the apparatus was removed from the glovebox. The reactor was charged with ethylene at 100 psi and kept at constant pressure. After 1 h the ethylene supply was closed and the reaction vessel was vented. The resulting polymer was washed with a methanol/7 M aqueous HCl (1:1) mixture followed by deionized water. The polymer was dried under vacuum at 90 °C for 18 h.

Acknowledgment. This research was supported by a grant from the National Science Foundation (Grant No. CHE-0132017).

Supporting Information Available: Tables giving X-ray crystallographic data. These data are available free of charge via the Internet at <http://pubs.acs.org>.

OM060514S

(33) Sheldrick, G. M. *SHELXTL*, version 6.01; University of Göttingen: Germany, and Bruker-AXS, Inc.: Madison, WI, 2001.

(34) Spek, A. L. *J. Appl. Crystallogr.* **2003**, *36*, 7.